RESEARCH

Evaluation on electrochemical properties of lithium-ion battery–based PMMA-PLA blend incorporation of [EDIMP] TFSI hybrid gel polymer electrolyte

N. F. Mazuki[1] · M. Z. Kufian[2] · A. S. Samsudin[1]

Abstract

This study focuses on developing a novel hybrid gel polymer electrolyte (HGPE) for lithium-ion batteries. The HGPEs comprise a hybrid polymer of polymethyl methacrylate (PMMA) and polylactic acid (PLA), doped with 20 wt.% lithium bis (trifluoromethylsulfonyl) imide salt (LiTFSI) and incorporated with various contents of ionic liquid, namely ethyl-dimethyl-propylammonium bis(trifluoromethylsulfonyl)imide ([EDIMP]TFSI) is successfully prepared, and the lithium-ion batteries performance was investigated. This work aims to investigate the influence of the ionic liquid on the electrical properties, cation transference number (t_{Li}^+), electrochemical stability window, and charge-discharge performance of the PMMA-PLA based HGPE systems. Among the different samples tested, the HGPE containing 20 wt.% [EDIMP]TFSI (E-TFSI 20) exhibited the most promising results. It achieved an optimum ionic conductivity of 3.90×10^{-3} S cm^{-1}, an increased t_{Li}^+ from 0.63 to 0.79, and an extended electrochemical stability window from 4.3 to 5V. Temperature dependence studies revealed that all the HGPE systems followed the Arrhenius characteristic, and their activation energies were calculated. Dielectric studies revealed ionic behavior and suitable capacitance with varying frequencies of the HGPEs system. The most favorable electrolyte was selected based on the highest ionic conductivity observed in each HGPE systems. It was utilized in a Li metal|HGPEs|graphite cell configuration. The discharge capacity of the cells using LiTFSI 20 and E-TFSI 20 electrolytes were measured as 152.06 mAh g^{-1} and 71.15 mAh g^{-1}, respectively, at a current density of 3.72 A g^{-1}.

Keywords Ionic liquid · Lithium transference number · Potential stability · Hybrid polymer

Introduction

Lithium-ion batteries (LIBs)–based organic liquid electrolyte has been widely employed in consumer and automotive applications. Although the high ionic conductivity of organic liquid electrolytes could potentially create a high energy density and cost-effective battery, it suffers from multiple fatal issues such as thermodynamically unstable, leakage, and flammability, which can lead to explosion [1, 2]. These problems have raised concern for the safety usage of LIBs among consumers. The development of polymer electrolytes has been widely investigated as a replacement for liquid electrolytes since their first discovery by Fenton in 1973 [3]. Polymer electrolytes are almost as promising as liquid electrolytes, with advantages such as easy processability, safety security, good mechanical flexibility, and high ionic conductivity [4–8].

Polymer electrolytes need to meet specific requirements to be suitable for use as electrolytes in LIBs. These requirements include (a) high room temperature ionic conductivity ($\leq 10^{-3}$ S cm^{-1}), (b) significant ionic transference number, (c) excellent mechanical strength, (d) broad electrochemical stability, and (e) sufficient dimensional stability to function as separators in batteries [9–11]. The first reported solid-state polymer electrolytes based on polyethylene oxide (PEO) and alkali metal salts have been found to exhibit low ionic conductivity [12]. This limitation has prompted research into gel polymer electrolytes (GPEs) as an intermediate state between liquid and solid electrolytes.

✉ A. S. Samsudin
ahmadsalihin@umpsa.edu.my

[1] Ionic Materials Team, Faculty of Industrial Sciences and Technology, Universiti Malaysia Pahang Al-Sultan Abdullah, 26300 Kuantan, Pahang, Malaysia

[2] Centre for Ionics University of Malaya, Department of Physics, Faculty of Science, Universiti Malaya, 50603 Kuala Lumpur, Malaysia

Research into GPEs was pioneered in 1975 by Feuillade and Perche [13], who examined the electrochemical properties of Li||CuS cells while employing various GPE formulations. GPEs can potentially enhance both safety and ionic conductivity, addressing the limitations of traditional solid-state polymer electrolytes [14]. GPEs are also believed to be the most suitable to act as separators in batteries as they comprise polymer matrix, lithium salt, and plasticizer/ionic liquid. In GPEs, the addition of plasticizers has swollen the polymer matrix in liquid electrolytes, leading them to achieve both the characteristics of solid and liquid electrolytes, giving them advantages in device applications [15].

Several promising supporting polymer matrix systems have been explored to prepare high-performance GPEs [16–20]. Among approaches that have been developed, polymer blending was chosen and prepared through dissolution solution technique. This method is a simple and versatile procedure to prepare various polymer matrices to facilitate ion transport. From our previous work, we found that blending polymethyl methacrylate (PMMA) and polylactic acid (PLA) using a composition weight ratio of 80:20 could contribute more vacancies for ion transportation in polymer matrix, which results in the enhancement of ionic conductivity from $\leq 10^{-12}$ S cm^{-1} (pure PMMA) to 10^{-6} S cm^{-1} (PMMA-PLA hybrid polymer) to 10^{-3} S cm^{-1} (PMMA-PLA-20 wt.% LiTFSI HGPE) [21]. One of the crucial factors in determining the possible applications of GPEs in LIBs is the Li$^+$ cation contribution to the total charge transport in the electrolyte complexes. The low lithium-ion transference number (t_{Li}^+) of LIBs can limit their performance, defined as the proportion of ionic conductivity provided by the lithium ion rather than its counterion [22]. According to Zhao et al. [23], high t_{Li}^+ is better for electrolyte stability to the lithium sheet and battery rate performance. Tsao et al. [24] prepared a polymer membrane without and with the ionic liquid group–based gel polymer electrolyte using solution casting methods. They reported that adding ionic liquid can boost the t_{Li}^+ because of their ability to limit the transportation of anions in the electrolyte complexes, thereby providing good pathways for Li$^+$ ions. Thus, it is expected it will contribute to the excellent battery performance.

Furthermore, ionic liquids (ILs) have gained enormous attention among researchers due to their exciting and potentially practical physicochemical features, including excellent chemical and electrochemical stability, high operating voltage, non-flammability, low vapor pressure, and high ionic conductivity [25, 26]. ILs function as plasticizers, where they can increase the flexibility and deformability of the amorphous section of the host polymer matrix. Within this host polymer matrix, the presence of ILs facilitates the formation of a highly conductive pathway through the GPEs, and this phenomenon can be explained by percolation theory, where ILs essentially enable the creation of a connected network of pathways for the movement of ions. Moreover, ILs play a crucial role in enhancing the compatibility at the interface between the GPEs and the active materials. This improved compatibility forms a passive film, a protective layer, at the interface, which is essential for the efficient functioning of the materials [27].

In this study, we prepared homogeneous HGPEs, which are composed of PMMA, PLA, lithium bis (trifluoromethylsulfonyl) imide salt (LiTFSI), and ethyl-dimethyl-propylammonium bis(trifluoromethylsulfonyl)imide ([EDIMP]TFSI) as ionic liquid. [EDIMP]TFSI was chosen to be used in the preparation of HGPEs as they demonstrate favorable characteristics in polymer electrolytes, including high thermal stability with a decomposition temperature (T_d) reaching 320 °C, low viscosity at 20 °C (71.63 mm^2 s^{-1}), a broad electrochemical stability range, excellent ion transport capabilities, and compatibility with the polymer host [28, 29]. The HGPEs have been prepared by dissolution solution method. Electrical impedance spectroscopy (EIS) was employed to measure the electrical properties of the HGPE systems. The lithium-ion (Li$^+$) transference number was determined by combining AC impedance measurements with DC polarization techniques. Additionally, linear sweep voltammetry (LSV) was utilized to ascertain the electrochemical stability window of the HGPE systems. It was found that adding IL to the PMMA-PLA-LiTFSI-based HGPE systems increased the t_{Li}^+ and extended the potential window stability of the electrolyte. The cycles' performance of the Li|LiTFSI 20|graphite and Li|E-TFSI 20|graphite cells has been investigated at different current densities of 3.72 and 11.16 A g^{-1}.

Experimental

Preparation of hybrid gel polymer electrolytes with incorporation of IL

The components of HGPE are PMMA (M.W. 996000 g/mol; Aldrich Co.), PLA (M.W. 120000 g/mol; Shandong Zhi Shang Chemical Co. LTD), LiTFSI (Aldrich Co.), and [EDIMP]TFSI (Sigma Aldrich Co.), which are known as non-flammable and non-volatile; ionic liquids, in particular, have low vapor pressure and high safety performance, as can be seen in Fig. 1. The solution casting method prepared hybrid gel polymer electrolytes containing [EDIMP]TFSI. The 0.04 g PLA was first dissolved in the 0.8 ml tetraethylene glycol dimethyl ether (TEGDME) at 120 °C. After a clear solution was obtained, the solution was cooled at room temperature before adding it with 20 wt.% LiTFSI salt and various amounts of [EDIMP]TFSI (5 to 35 wt.%). The solution was continued to stir until it completely dissolved. Lastly, 0.16 g PMMA polymer was added to the solution and continued stirring at 70 °C. The polymer solution was

again left at room temperature and stirred vigorously until the uniform and viscous solution was obtained. The HGPEs have been stored under an argon atmosphere before future analysis. The sample preparation and designation of HGPEs are demonstrated in Fig. 1.

Preparation of graphite anode

The graphite anode was fabricated by applying a slurry onto a graphite sheet. The slurry was composed of a mixture of graphite, super P, and poly(vinylidene fluoride) (PVDF) binder in N-methyl pyrrolidone (NMP) solvent, with a weight ratio of 80:10:10. The graphite sheet was initially cut to match the size of the coin cell. Then, the slurry was applied using a dropping technique. The electrode was subsequently dried in a vacuum oven at 120°C overnight.

Characterization of HGPE-based IL

Electrical measurement

In the present work, impedance spectroscopy was employed to determine the ionic conductivity. The HGPE was placed between two stainless steel (SS) electrodes within a coin cell configuration of SS|HGPEs|SS. Impedance measurements were conducted using a HIOKI 3532-50 LCR Hi-TESTER, applying an AC amplitude of 10 mV. The frequency range for the measurements spanned from 1 MHz to 50 Hz. The influence of temperature on the ionic conductivity of the HGPEs was carried out across a temperature range of 303 to 393 K for each sample.

Cation transference number measurement

The lithium-ion transport number of hybrid gel polymer electrolytes was measured using a Li|HGPEs|Li cell configuration, where lithium metal acted as non-blocking electrodes. The methodology described was determined according to the method described by Evans [30] to calculate t_{Li}^+, which involved a combination of DC potentiostat measurements and AC impedance spectroscopy. To begin, the HGPEs was polarized at 100 mV using DC polarization. The polarization process could be characterized by measuring the initial current (I_o) and steady-state current (I_{ss}). Subsequently, impedance spectroscopy was performed over a frequency range of 100 kHz to 10 mHz to analyze the film resistance of the HGPEs before (R_o) and after (R_{ss}) the polarization tests. By integrating the data obtained from both measurements, the t_{Li}^+ was calculated using a specific relation:

$$t_{Li^+} = \frac{I_{ss}(\Delta V - I_o R_o)}{I_0(\Delta V - I_{ss}R_{ss})} \qquad (1)$$

where ΔV is the applied voltage across the HGPEs during DC polarization. This approach allowed for the

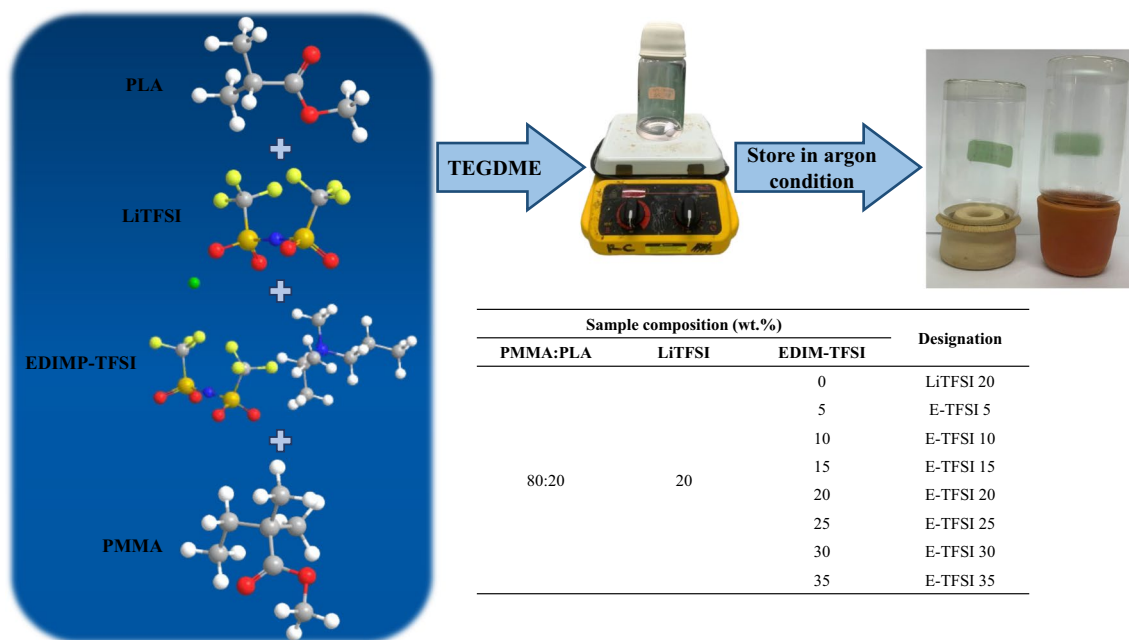| Sample composition (wt.%)			Designation
PMMA:PLA	LiTFSI	EDIM-TFSI	
		0	LiTFSI 20
		5	E-TFSI 5
		10	E-TFSI 10
80:20	20	15	E-TFSI 15
		20	E-TFSI 20
		25	E-TFSI 25
		30	E-TFSI 30
		35	E-TFSI 35

Fig. 1 Schematic diagram of HGPE preparation using dissolution solution method and its designation

determination of t_{Li}^+ and its contribution to the overall behavior of the HGPEs.

Linear sweep voltammetry

The electrochemical stability of HGPEs was investigated using linear sweep voltammetry. For this purpose, coin cells were assembled with HGPE samples sandwiched between SS electrodes as the working electrodes, while lithium metal served as the counter and reference electrode. The assembly process was conducted within an inert dry box. During the experiments, the scan rate was set to 10 mV s^{-1}, and the electrochemical behavior of the HGPEs was analyzed through the applied voltage sweep. It allowed for assessing the HGPE's electrochemical stability and provided insights into its performance under varying voltage conditions from 2.8 to 6.5 V.
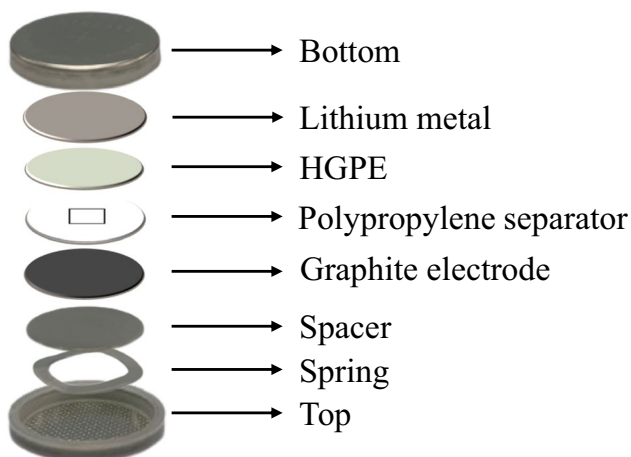

Fig. 2 Arrangement of half-cell graphite electrode

Cell fabrication and battery testing

For the assembly of the half-cell lithium-ion battery, the highest conducting HGPE samples were placed between the graphite anode and the lithium-metal cathode, as illustrated in Fig. 2. All the cell assembly procedures were conducted within a dry box filled with argon gas to ensure a controlled and moisture-free environment.

The coin cell configuration used in this study was Li metal|HGPEs|graphite, where the lithium metal acted as the anode, the HGPEs served as the electrolyte, and graphite was used as the cathode material. CR 2032 coin cell holders were used as the packaging cell in the present system. The charge-discharge performance of the cells was evaluated under two different current densities: 3.72 A g^{-1} and 11.16 A g^{-1}. The tests involved cycling the cells between 0.01 and 2 V for 10 cycles. These experiments allowed for examining the cell's performance, capacity retention, and cycling stability under different operating conditions.

Result and discussion

Ionic conduction properties studies

Figure 3 presents the frequency dependence of the AC conductivity for the HGPEs with and without ionic liquid (IL) at room temperature. The plot reveals two distinct regions characterized by different conductivity behaviors. The low-frequency dispersive region is attributed to electrode polarization effects at the blocking electrodes. At lower frequencies, a significant amount of charge accumulates at the interface between the electrode and the electrolyte. This accumulation reduces the mobility of ions, consequently leading to a decrease in conductivity. Meanwhile, the frequency-independent plateau region represents the DC conductivity. At
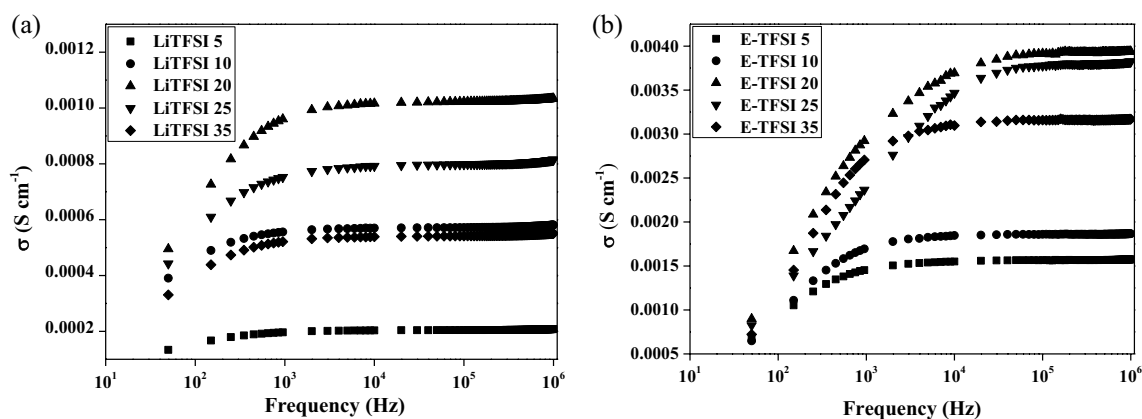

Fig. 3 Variation of AC conductivity with frequency of (**a**) PMMA-PLA-LiTFSI- and (**b**) PMMA-PLA-LiTFSI-IL-based HGPEs at room temperature

higher frequencies, the period of the applied field is too short for significant charging to occur at the electrode-electrolyte interface. As a result, the AC conductivity tends to stabilize and assume a frequency-independent value equivalent to the DC conduction. By extrapolating the DC plateau on the conductivity axis, the DC conductivity of the system can be determined. This extrapolation allows for estimating the conductivity under steady-state conditions, providing valuable insights into the material's overall conductive properties [31].

It also can be seen from Fig. 3(a) that the DC conductivity increases from 10^{-4} S cm^{-1} optimum value of 1.02×10^{-3} S cm^{-1}, corresponding to a sample containing 20 wt.% of LiTFSI. This phenomenon might be due to the number of charge carriers increased by dissociating ion pairs and ion aggregates [Li$^+$---TFSI$^-$] that improve ionic conductivity. The highest conducting sample from PMMA-PLA-LiTFSI (LiTFSI 20) HGPEs was chosen for further improvement by adding various content of IL, namely [EDIMP]TFSI as illustrated in Fig. 3(b). It was shown from the figure that the ionic conductivity raised to 3.90×10^{-3} S cm^{-1} with an increase of IL content up to 20 wt.% [EDIMP]TFSI (E-TFSI 20). The possible reason for such behavior can be discussed due to the increment in mobile charge species generation by the IL. The IL contains mobile EDIMP$^+$ and TFSI$^-$ ions, thereby augmenting the pool of charge carriers responsible for conduction. The increased ionic conductivity observed in the HGPEs can be attributed to the exceptional self-dissociation and ion transport properties demonstrated by [EDIMP]TFSI. This indicates that [EDIMP]TFSI can dissociate and transport ions effectively, thereby enhancing ionic conductivity in the HGPEs system [32].

Moreover, the incorporation of the IL into the system introduced supplementary pathways that facilitated the movement of ions along the surface of the polymer matrix. This additional network of pathways contributed to the enhanced ion mobility within the hybrid polymer matrix [33]. It was made possible by the proximity of the ions to each other. As a result, the mobile charge carriers could migrate within the polymer matrix. Moreover, the Li$^+$ and TFSI$^-$ ions could also migrate, leading to increased ionic conductivity due to their enhanced mobility [34]. In addition, the ionic liquid has a plasticization effect on the system, resulting in increased flexibility of the polymer chains. This enhanced flexibility promotes the movement of ions within the polymer backbone, thereby contributing to improved ion conductivity [35]. However, it should be noted that beyond a 20 wt.% content for both systems, the ionic conductivity starts to decrease. This decrease can be attributed to the restricted movement of ions within the rigid polymer matrix due to overcrowding of ions, leading to sample crystallization [16, 36]. Khurana et al. [37] and Chaurasia et al. [38] also agreed that the elevation in the content of added ionic species has resulted in the formation of a considerable amount of ion pairs within the polymer electrolyte. In turn, it reduces the availability of free mobile charge carriers responsible for conduction in the hybrid electrolyte, leading to a decline in ionic conductivity.

The temperature dependence of electrical conductivity was investigated across a range from ambient temperature to 393K and presented in Fig. 4. Figure 4(a) depicts the temperature-dependent conductivity for the PMMA-PLA-based hybrid polymer electrolytes with varying LiTFSI contents. At the same time, Fig. 4(b) illustrates the conductivity for different [EDIMP]TFSI contents. In both figures, no significant or abrupt changes in ionic conductivity were observed as the temperature increased. This absence of sudden changes suggests the absence of phase transitions within the investigated temperature range for all the polymer electrolyte complexes. The smooth and gradual changes in conductivity with temperature indicate a continuous and stable ionic conduction mechanism throughout the temperature range studied [39, 40].
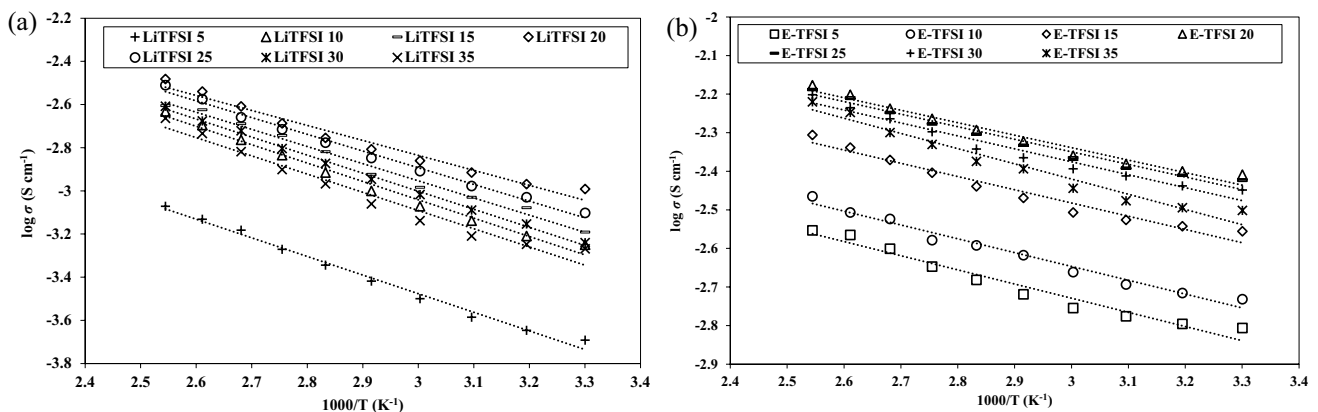

Fig. 4 Temperature dependence studies of (**a**) LiTFSI various content and (**b**) [EDIMP]TFSI various content at 303 to 393K

In both cases, an increase in ionic conductivity with temperature was observed, which can be attributed to the expansion of the polymer matrix. This expansion creates additional free volume and empty spaces, providing pathways for ion migration. It is important to note that this phenomenon indicates the decoupling of charge carriers in the HGPEs from the segmental motion of the polymer chains. As a result, ion transport primarily occurs through the gel electrolyte rather than along the polymeric chains [41]. This behavior is commonly observed in liquid electrolytes and gel-type polymer electrolytes. Furthermore, as the temperature rises, the vibrational energy of polymer segments becomes sufficient to overcome the hydrostatic pressure imposed by neighboring atoms. It allows the segments to create small regions of increased space, enabling enhanced vibrational motion. Consequently, the ionic conductivity increases with temperature. The difference in ionic conductivity values between Fig. 4(a) and Fig. 4(b) can be attributed to the appearance of new ionic carrier mobilities, such as [Li$^+$---TFSI$^-$] and [Li$^+$---TFSI$^-$, EDIMP$^+$---TFSI$^-$], respectively. The regression values being close to unity suggest that the temperature-dependent ionic conductivity of both HGPEs system, with and without IL, follows the Arrhenius characteristic. This empirical relationship has been reported in previous studies and provides a suitable description of the conductivity behavior with changing temperatures [42–44].

Table 1 presents the Arrhenius parameters for the HGPEs system based on PMMA-PLA-LiTFSI and PMMA-PLA-LiTFSI-IL. In the HGPEs, the Li$^+$ ions dissociate from the polymer chain, allowing other Li$^+$ ions from the surrounding environment to occupy the vacant sites with segmental motion. The movement and coordination of Li$^+$ ions within the polymer complex require energy, referred to as activation energy (E_a). It is noticeable from the table that E_a values for both systems reveal relatively low and almost constant for different sample contents. According to Dissanayake et al. [45], the activation energy for ion transport in organic solution electrolytes appears to be primarily influenced by the solvent family rather than salt concentration or type, suggesting its dependence on the nature of the solvent's heteroatom. This activation process is likely

associated with dipole re-orientation related to the solvent's functional group, contrasting with solid electrolytes where ion transport involves thermally activated hopping between occupied and vacant sites. Previous research on gel polymer electrolyte systems has reported similar findings to the current study, demonstrating consistency in the observed trends [46, 47]. In addition, the table indicates that as the content of both LiTFSI and [EDIMP]TFSI increases, the E_a values decrease. For PMMA-PLA-LiTFSI, E_a decreases from 7.18 to 5.78 kJ mol^{-1}, while for PMMA-PLA-LiTFSI-IL, E_a decreases from 3.07 to 2.69 kJ mol^{-1}. This decrement pattern can be explained by the introduction of lithium salt and IL, which leads to an increased amorphous region within the polymer matrix. The presence of the amorphous phase implies that the arrangement of particles in the polymer matrix is less organized. This arrangement allows the attractive bonds between molecules to break more easily, requiring less energy for ion hopping and coordination with the ester group of the hybrid polymer [48]. It can be concluded that the hopping process is more favorable with a lower E_a value, indicating that a lower E_a value corresponds to higher ionic conductivity in the PMMA-PLA hybrid polymer when LiTFSI is used as a dopant salt and [EDIMP]TFSI is employed as the IL.

The dielectric permittivity of the HGPEs was investigated to evaluate their capacity for storing and losing electrical energy in an electric field. Figure 5 presents the dielectric constant (ε_r) and dielectric loss (ε_i) as a function of different LiTFSI and [EDIMP]TFSI contents in the HGPEs at selected frequencies. The figures indicate that both dielectric permittivity parameters increase with the addition of lithium salt and IL to the hybrid polymer systems, enhancing the HGPE's ability to store and dissipate electrical energy. This increment in dielectric permittivity can be attributed to the increased density of charge carriers provided by LiTFSI and [EDIMP]TFSI, enabling the charges to move within the polymer chain and contribute to its electrical conductivity [32, 49]. The correlation between dielectric permittivity (ε_r and ε_i) and conductivity of materials has been widely established. An increase in the ε_r and ε_i of materials commonly leads to an elevation

Table 1 List of ionic conductivity, σ, regression value, R^2, and activation energy, E_a, for HGPEs system with and without IL

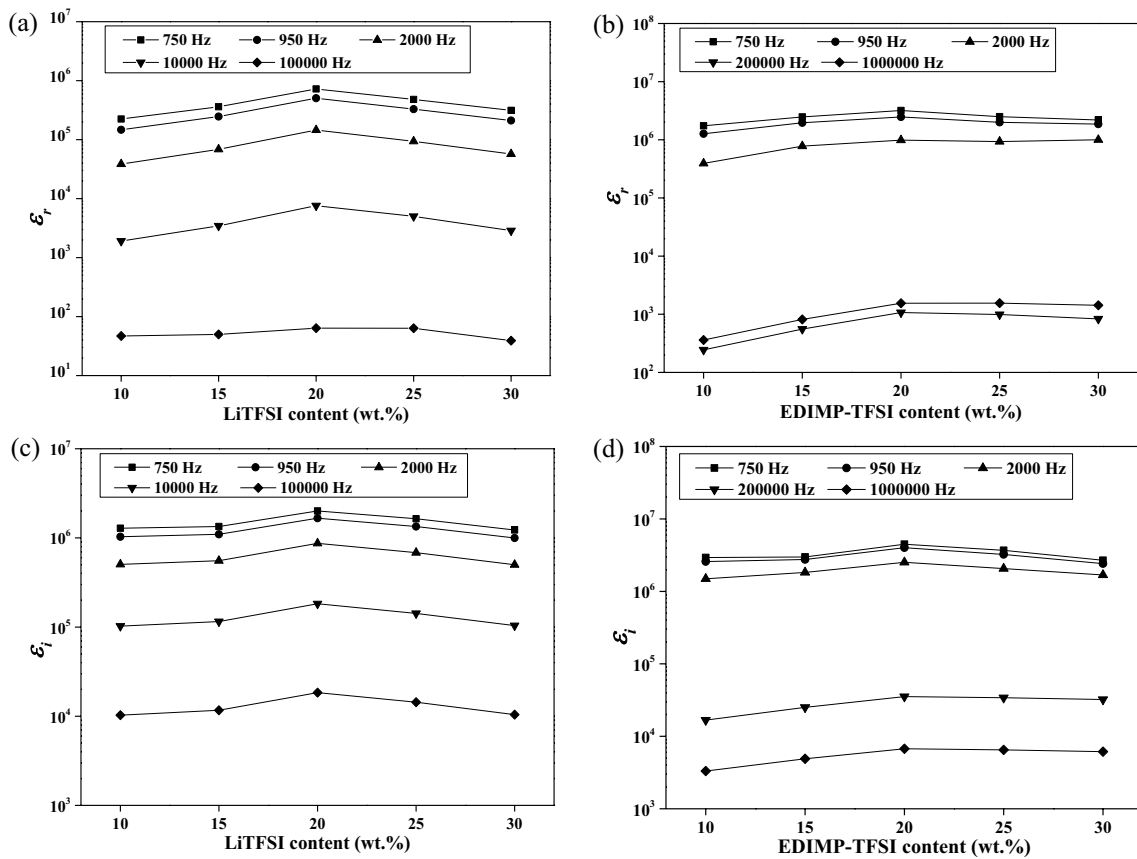| wt.%	LiTFSI			[EDIMP]TFSI		
	σ (S cm^{-1})	R^2	E_a (kJ mol^{-1})	σ (S cm^{-1})	R^2	E_a (kJ mol^{-1})
5	2.03×10^{-4}	0.99	7.18	1.56×10^{-3}	0.96	3.07
10	5.63×10^{-4}	0.99	7.08	1.86×10^{-3}	0.98	2.98
15	6.45×10^{-4}	0.99	6.61	2.78×10^{-3}	0.96	2.85
20	1.02×10^{-3}	0.97	5.78	3.90×10^{-3}	0.97	2.69
25	7.90×10^{-4}	0.99	6.45	3.77×10^{-3}	0.98	2.71
30	5.75×10^{-4}	0.99	6.97	3.56×10^{-3}	0.96	2.79
35	5.39×10^{-4}	0.97	7.02	3.15×10^{-3}	0.96	3.28

Fig. 5 Dielectric properties studies of HGPEs system for without and with IL (**a**) and (**b**) dielectric constant, and (**c**) and (**d**) dielectric loss at 303K, respectively

in ionic conductivity while simultaneously reducing electronic conductivity. This occurrence is attributed to the fact that a higher ε_r and ε_i signifies a greater capacity of the material to segregate and polarize charges. As a result, the movement of ions is facilitated.

Consequently, materials with higher ε_r and ε_i values are inclined to demonstrate more significant ionic conductivity due to improved ion mobility in an applied electric field, making it a critical parameter for optimizing their performance in battery applications [50]. Furthermore, the plots closely follow the trends observed in ionic conductivity, as discussed earlier. However, beyond 20 wt.% of LiTFSI and [EDIMP]TFSI, a decline in both ε_r and ε_i is observed. It can be explained by the reassociation of ions and the formation of neutral ion pairs, which reduces the number of charge carriers and consequently diminishes the HGPE's ability to store electrical energy [16, 51]. Another factor contributing to the decrease in ε_r and ε_i is the tendency of dipoles in the macromolecules to align themselves in the direction of the applied electric field, especially within the low-frequency range. This alignment of dipoles can limit the material's ability to store electrical energy [52].

Lithium-ion transport number studies

The transference number indicates the correlation between the surface polarity of materials and their ion transport property [53]. In addition, a higher Li$^+$ transport number can reduce concentration polarization during charge-discharge cycles and sustain the power density of the electrolyte [54, 55]. Therefore, the $t_{Li}{}^+$ of the highest conducting HGPEs sample, both with and without IL, was measured at room temperature. Incorporating [EDIMP]TFSI into the PMMA-PLA-LiTFSI complex significantly impacts the system's ionic conductivity, resulting in an increase in the total current involved and generated. This enhancement in conductivity can be attributed to the contribution of Li$^+$ ions in the polymer complexes. To measure the $t_{Li}{}^+$, the LiTFSI 20 and E-TFSI 20 samples were placed between lithium-metal electrodes, as illustrated in Fig. 6. Lithium-metal electrodes were chosen as non-blocking electrodes since the charge carriers in this HGPEs system are lithium ions (Li$^+$). This electrode configuration allows for the passage of Li$^+$ through the electrode, enabling the measurement of the number of Li$^+$ transports.
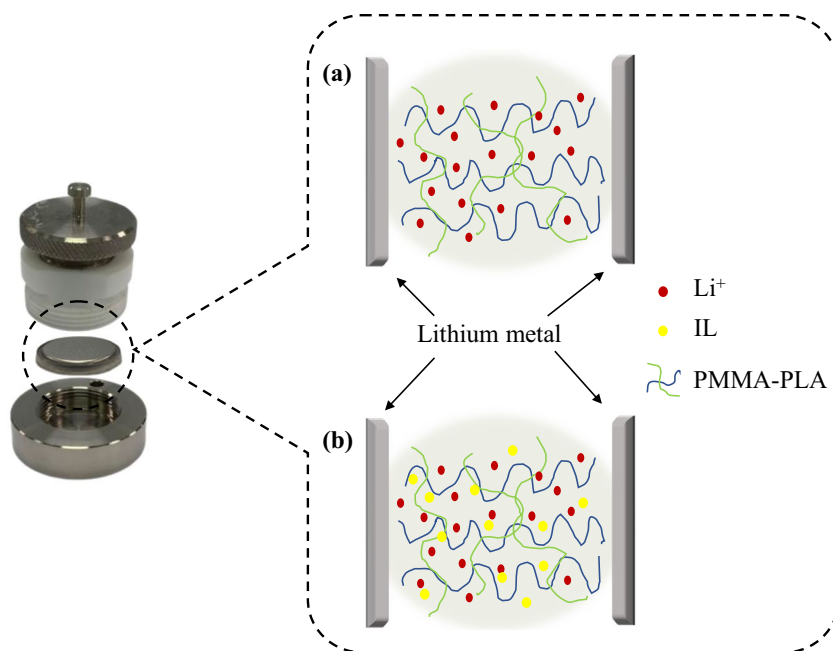
The t_{Li}^+ can be evaluated by measuring the final steady-state current (I_{ss}) and initial current (I_o) under a constant potential bias. For ideal electrolytes under negligible polarization voltage, the cations transport can be calculated as $t_{Li}^+ = I_{ss}/I_o$ [56]. However, there is a change in interfacial resistance that has occurred during impedance studies. In order to ensure the accuracy of the measurements, certain modifications to the method were implemented to account for the interface between the electrolyte and the lithium metal. Bruce and Vincent have introduced new techniques to determine the number of lithium-ion transports in polymer complex–based HGPEs by combining AC impedance

and DC polarization measurements [30, 57–59]. Before the DC polarization test, the AC impedance response of the Li|HGPE|Li cell was analyzed. A constant voltage pulse (ΔV) was applied to the cells until the polarization current reached a steady state, and subsequently, the impedance response of the cells was re-examined. A double AC measurement was employed to determine the resistances, measuring the resistance before (R_o) and after (R_{ss}) the DC polarization.

Figure 7 depicts the current polarization result of HGPEs system and the impedance plot (inset plot) at room temperature. The t_{Li}^+ of this study was calculated

Fig. 7 Lithium transference number of Li/HGPE/Li through DC polarization (red plot) and impedance analysis (inset figure) for (**a**) LiTFSI 20 and (**b**) E-TFSI 20
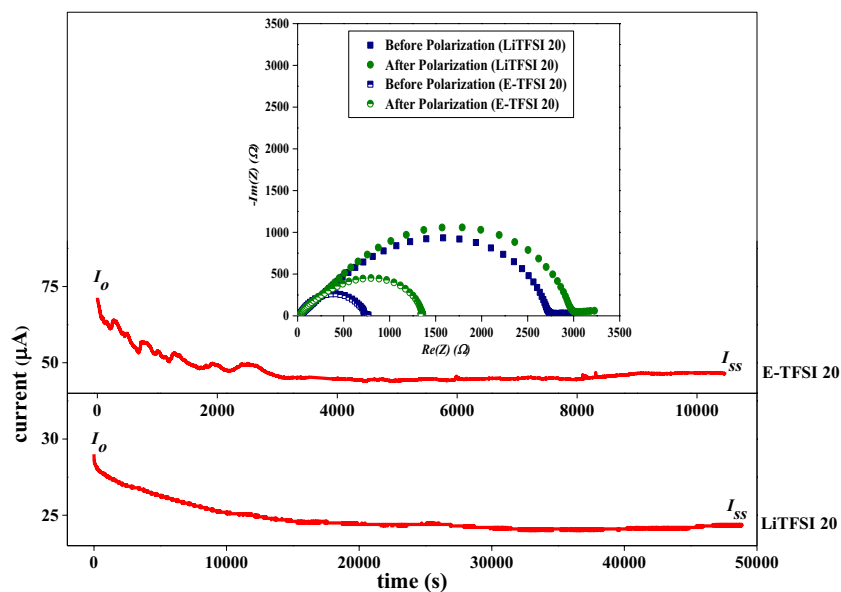
using parameters listed in Table 2 via Eq. (1), and it was found that the addition of IL into the HGPEs system has improved the t_{Li}^+ from 0.62 to 0.79. The enhancement of t_{Li}^+ to a higher number could be attributed to the strong electrolyte absorption (refers to the ability of the electrolyte to absorb and retain ions) through the cell and molecular interactions between the hybrid polymer and the charged ions (Li$^+$---TFSI$^-$ and EDIMP$^+$---TFSI$^-$) in the polymer complex [60]. It shows that adding [EDIMP] TFSI may favor the re-dissociation of ion pairs and weaken the interactions involving Li$^+$ and the functional group of hybrid polymer, thus boosting the number of free Li$^+$ ions [61]. This flexible and delocalized nature also facilitates the transport of Li$^+$ ions in the polymer backbone. However, according to Ghosh et al. [62], achieving a high transference number of lithium ions without any anion trapper additives is unexpected since they believed a large anion molecular size could influence the lithium-ion transport number. Meanwhile, Appetecchi et al. [63] claimed that the t_{Li}^+ can be achieved as high as 0.8 by studying the unique interaction between host polymer (PMMA or PAN), solvent (EC and PC), and lithium salt (LiTFSI). Furthermore, Shah et al. investigated the effect of anion size on transference number based on three different lithium salt (LiFSI, LiTFSI, and LiBETI). They found that the t_{Li}^+ was above 0.6 for all the electrolytes and was increasing function of anion size [64]. Moreover, Libo et al. reported t_{Li}^+ of LiTFSI-P(VdF-HFP)-based HGPE without and with IL revealed 0.8 for both systems [65]. Another finding was found with higher t_{Li}^+ of 0.76 and 0.62 based on a hybrid gel polymer electrolyte system reported by Li et al. [66] and Isa et al. [67], respectively. Hence, it can be concluded that the present results are compatible with previous studies.

Electrochemical stability window studies

It is crucial to investigate its electrochemical stability and its interactions with the electrodes in lithium-ion batteries to ensure the suitability of electrolyte material for practical battery devices. As many lithium-based electrode chemistries operate at high voltages, the electrolyte material needs to possess a wide electrochemical stability window that extends beyond the operating potential of the electrodes. The battery needs to function effectively within the typical temperature range of approximately 40 to 60 °C [68]. A linear sweep voltammetry test was performed to assess the potential window stability of the HGPEs. Figure 8 illustrates the linear sweep voltammograms of the HGPEs sample LiTFSI 20 and E-TFSI 20 at a scan rate of 10 mV s^{-1}. The plots reveal that the sudden increase in current during the potential sweeping towards anodic values signifies the anodic decomposition voltage of the HGPEs. It also can be seen that the HGPE with the presence of IL exhibited a potential stability of 5 V, which is greater than HGPE without IL with 4.3 V at room temperature. The enhancement of the decomposition voltage of the HGPE with the addition of IL into the system can be elucidated due to the formation of a stable passive layer and electrolyte decomposition at the inert electrode interface [69–71]. It is worth noting that a stable passive layer enhances the potential window by providing a protective barrier that prevents unwanted reactions and ensures

Table 2 Parameter of lithium transport measurement of HGPEs

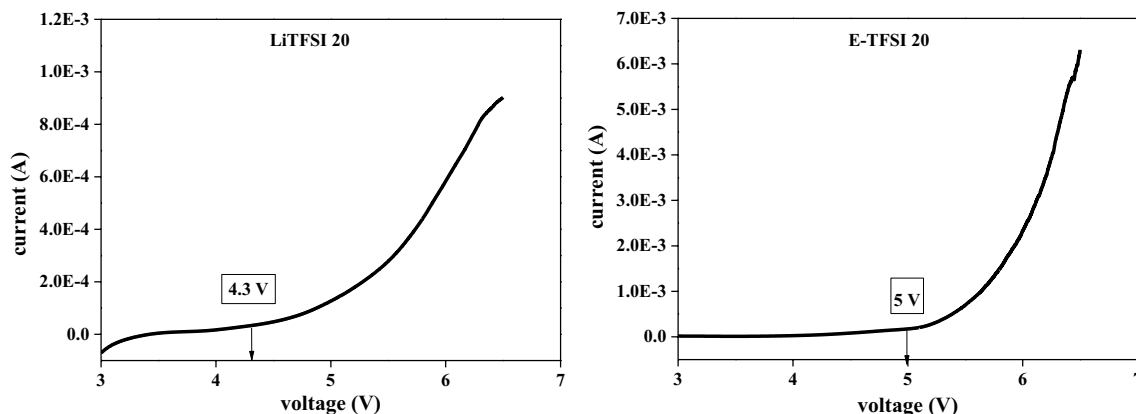| Sample	R_o (Ω)	R_{ss} (Ω)	I_o (μA)	I_{ss} (μA)	Voltage (V)	t_{Li}^+
LiTFSI 20	2.74×10^3	2.98×10^3	29.0	24.3	0.1	0.62
E-TFSI 20	7.70×10^2	1.36×10^3	71.3	46.4	0.1	0.79

Fig. 8 Electrochemical stability curve of HGPEs at room temperature

the stability of the electrochemical system, allowing for a broader range of operating voltages and improving overall performance and reliability [72]. In addition, the formation of an anodic stability window is believed to correlate with an irreversible oxidation of the salt anion [73]. This analysis provides insights into the ability of the electrolyte to withstand higher voltages, which is essential for the stable operation of lithium-ion batteries.

Charge-discharge profile studies

The PMMA-PLA-20 wt.% LiTFSI and PMMA-PLA-20 wt.% LiTFSI-20 wt.% IL hybrid gel polymer electrolytes are tested in Li/graphite half-cell lithium-ion batteries at room temperatures. Figure 9 shows the charge-discharge curves of Li|HGPE|graphite cells at the first cycle with a different current density of 3.72 A g^{-1} and 11.16 A g^{-1}. The cut-off potential for charging and discharging are 2.0 and 0.01 V, respectively. It can be noticed from Fig. 9 that the current work does not show profiles as standard graphite anode profiles. According to the literature, this issue could have several possible reasons. They include (a) surface contamination that could affect the intercalation and deintercalation processes of lithium ions in the graphite structure, (b) structural defects that affect lithium-ion diffusion and intercalation, (c) electrolyte materials effects on the interfacial processes, lithium-ion solvation, or solid-electrolyte interface (SEI) formation, and (d) cycling conditions, including the voltage range, current density, and temperature [74–76]. However, in this work, we believed chemical reactions happened during the charge-discharge process examined from the charge-discharge profiles.

It can be observed that the cycling profiles at 3.72 A g^{-1} and 11.16 A g^{-1} for Li|LiTFSI 20|graphite cell show small changes compared to Li|E-TFSI 20|graphite cell. The phenomenon of electrode activation polarization, which refers to changes in charge-discharge profiles, occurs due to the slower lithiation kinetics of the electrode at higher current densities [77]. In simpler terms, when the current density increases, the electrode's capacity to absorb lithium ions becomes limited, leading to decreased capacity and efficiency. It is a well-known challenge in lithium-ion batteries. It is primarily caused by the aging process of the anode electrode and the formation of the solid-electrolyte interface (SEI) layer. These factors contribute to the loss of active lithium within the battery system [78].

Figure 10 illustrates the discharge performance curves of the Li|HGPE|graphite cell at the current density of 3.72 A g^{-1}. It can be seen from the figure the first discharge capacity for Li|LiTFSI 20|graphite and Li|E-TFSI 20|graphite cells is 152.06 mAh g^{-1} and 71.15 mAh g^{-1}, respectively. It is worth noting that the performance of the graphite anode with the
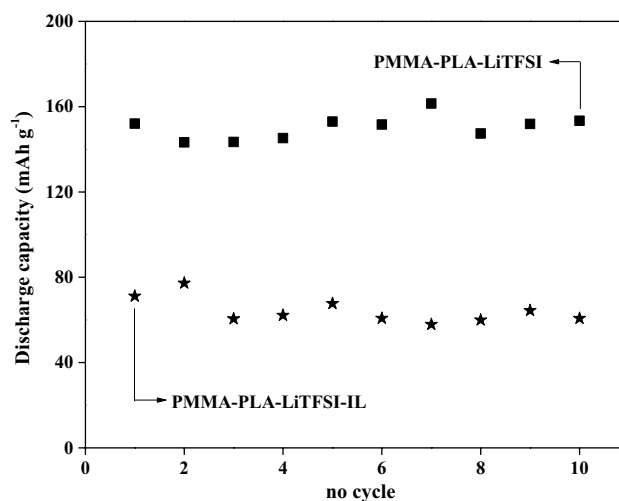

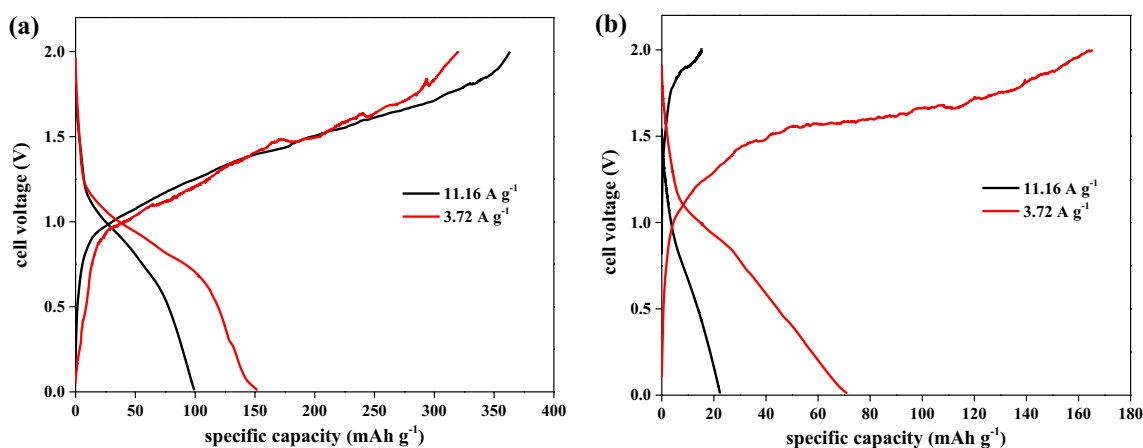**Fig. 10** Discharge capacity versus number of cycles for HGPE systems at 3.72 A g^{-1}

Fig. 9 Galvanostatic charge-discharge curves of Li/graphite half cells with (**a**) LiTFSI 20 and (**b**) E-TFSI 20 HGPE at different current densities

Table 3 Previous study on half-cell lithium-ion batteries–based GPEs

GPE	Electrode material	σ (s cm^{-1})	C_{sp} (mAh g^{-1})	References
AMS terpolymer/LiClO$_4$/EC/DMC/silica	Graphite	5.10×10^{-4}	305	[82]
PVDF-HFP/trilayer polypropylene/SiO$_2$	Graphite	1.00×10^{-2}	349/347.18	[83]
P(MA-co-AN)/PVA/LiPF$_6$/EC/DMC/DEC	Graphite	0.98×10^{-3}	307	[84]
PMMA-PLA-LiTFSI	Graphite	1.02×10^{-3}	152.06	Current work
PMMA-PLA-LiTFSI-[EDIMP]TFSI	Graphite	3.90×10^{-3}	71.15	Current work

addition of IL was initially lower than without IL, which is not as expected since IL shows the highest ionic conductivity performance as an electrolyte. In a study conducted by Chatterjee et al. [79], they examined the cycling performance of lithium-ion battery cells in a half-cell configuration, both with and without the addition of an IL additive. Surprisingly, the cells without IL additives performed better, especially during the initial cycles. They hypothesized that this disparity in performance could be linked to the degradation of the electrolyte on the graphite electrode, a phenomenon potentially caused by the presence of the IL. This degradation was associated with the IL having a lower energy level in its lowest unoccupied molecular orbital (LUMO), suggesting that the IL might contribute to adverse reactions at the electrode-electrolyte interface, impacting the battery's overall performance [79].

Moreover, it is widely recognized that the electrolyte plays a crucial role in facilitating the movement of lithium ions between the electrodes in lithium batteries. The addition of IL in the HGPE systems may have interacted with the electrolyte and affected its stability or reactivity. It is suggested that the addition of IL caused degradation of the electrolyte on the graphite electrode. In another study by Liu et al. [80], it was highlighted that ionic liquid electrolytes based on bis(trifluoromethanesulfonyl)imide (TFSI) and lithium salt, although demonstrating excellent cycling performance for lithium batteries, do not perform effectively in Li-ion batteries. This limitation is primarily attributed to the behavior of the cations present in these ionic liquids, which tend to undergo severe intercalation and reductive decomposition in graphite before the Li$^+$ ions during the initial cycle. In other words, the cations in TFSI-based ionic liquids react with graphite before the lithium ions can, limiting their performance in Li-ion batteries. Wang et al. [71] also agreed that ionic liquid–based electrolytes cannot form a stable SEI layer between the electrode and electrolyte. This is crucial for battery performance, especially in cycle performance. Table 3 presents the performance of lithium-ion batteries using a gel polymer electrolyte system comprising lithium salt and ionic liquid, as reported in the literature. Based on the information provided in the table, it can be inferred that the current findings for the LiTFSI 20 and E-TFSI 20 systems exhibit discharge capacities that are very low compared to those reported in previous studies based on graphite anode. Armand et al. [81] suggest that research efforts are primarily focused on lithium-metal batteries rather than lithium-ion batteries when it comes to using ionic liquid–based GPEs. This preference arises from the superior compatibility of these GPEs with high-capacity lithium-metal anodes, making them a more promising choice for advancing the development of next-generation energy storage technologies. Therefore, further investigation on the HGPE's materials and electrode's materials is highly recommended for better performance in practical application.

Conclusion

A new HGPEs system–based PMMA-PLA-LiTFSI-[EDIMP] TFSI was successfully developed for lithium-ion batteries. Introducing ionic liquid into the systems has improved the electrolytes' performance in ionic conduction and electrical properties. Sample E-TFSI 20 shows the optimum ionic conductivity of 3.90×10^{-3} S cm^{-1}, corresponding to the lowest E_a value. The temperature-dependent study on all HGPE systems demonstrated adherence to Arrhenius behavior, where the ionic conductivity increased with temperature without sudden decline. Incorporating the IL ([EDIMP]TFSI) into the HGPE resulted in an increase in both the lithium-ion transference numbers (from 0.62 to 0.79) and the electrochemical stability (from 4.3 to 5 V) for LiTFSI 20 and E-TFSI 20 samples. Regarding lithium-ion battery performance, it can be inferred that using the ionic liquid–based [EDIMP]TFSI is incompatible with the graphite anode. This incompatibility led to potential chemical reactions occurring at the interface between the electrode and electrolyte, thereby impeding the movement of Li$^+$ ions during the charge-discharge process.

Author contributions N.F. Mazuki: Writing – original draft, Methodology, Investigation, Writing – review & editing. M.Z. Kufian: Supervision, Formal analysis, Writing – review & editing. A.S. Samsudin: Writing – review & editing, Validation, Conceptualization, Funding acquisition, Supervision, Visualization.

Declarations

Competing Interest The authors declare the following financial interests/personal relationships which may be considered as potential competing interests: A.S. SAMSUDIN reports financial support, equipment, drugs, or supplies, and statistical analysis were provided by Universiti Malaysia Pahang Al-Sultan Abdullah. A.S. SAMSUDIN reports financial support was provided by Universiti Malaysia Pahang Al-Sultan Abdullah.

References

1. Niu H, Wang L, Guan P, Zhang N, Yan C, Ding M, Guo X, Huang T, Hu X (2021) Recent advances in application of ionic liquids in electrolyte of lithium ion batteries. J Energy Storage 40:102659

2. Chang X, Zhao Y-M, Yuan B, Fan M, Meng Q, Guo Y-G, Wan L-J (2023) Solid-state lithium-ion batteries for grid energy storage: opportunities and challenges. Sci China Chem:1–24

3. Fenton DE (1973) Complexes of alkali metal ions with poly (ethylene oxide). Polym 14:589

4. Rollo-Walker G, Malic N, Wang X, Chiefari J, Forsyth M (2021) Development and progression of polymer electrolytes for batteries: influence of structure and chemistry. Polym 13(23):4127

5. Ngai KS, Ramesh S, Ramesh K, Juan JC (2016) A review of polymer electrolytes: fundamental, approaches and applications. Ionics 22(8):1259–1279

6. Nishshanke G, Arof A, Bandara T (2020) Review on mixed cation effect in gel polymer electrolytes for quasi solid-state dye-sensitized solar cells. Ionics 26:3685–3704

7. Arya A, Sharma A (2017) Polymer electrolytes for lithium ion batteries: a critical study. Ionics 23(3):497–540

8. Singh P, Sachdeva A, Bhargava C (2022) Polymer electrolyte a novel material for electrochemical devices: a review. In: Journal of Physics: Conference Series. IOP Publishing, p 012021

9. Cheng X, Pan J, Zhao Y, Liao M, Peng H (2018) Gel polymer electrolytes for electrochemical energy storage. J Adv Energy Mater 8(7):1702184

10. Zhou D, Shanmukaraj D, Tkacheva A, Armand M, Wang G (2019) Polymer electrolytes for lithium-based batteries: advances and prospects. Chem 5(9):2326–2352

11. Bocharova V, Sokolov AP (2020) Perspectives for polymer electrolytes: a view from fundamentals of ionic conductivity. Macromolecules 53(11):4141–4157

12. Fenton D (1973) Complexes of alkali metal ions with poly (etylene oxide). Polym 14:589

13. Feuillade G, Perche P (1975) Ion-conductive macromolecular gels and membranes for solid lithium cells. J Appl Electrochem 5(1):63–69

14. Baskoro F, Wong HQ, Yen H-J (2019) Strategic structural design of a gel polymer electrolyte toward a high efficiency lithium-ion battery. ACS Appl Energy 2(6):3937–3971

15. Maheshwaran C, Mishra K, Kanchan D, Kumar D (2020) Mg^{2+} conducting polymer gel electrolytes: physical and electrochemical investigations. Ionics 26:2969–2980

16. Prasanna CS, Suthanthiraraj SA (2018) Dielectric and thermal features of zinc ion conducting gel polymer electrolytes (GPEs) containing PVC/PEMA blend and EMIMTFSI ionic liquid. Ionics 24:2631–2646

17. Ramesh S, Liew C-W, Ramesh K (2011) Evaluation and investigation on the effect of ionic liquid onto PMMA-PVC gel polymer blend electrolytes. J Non-Cryst Solids 357(10):2132–2138

18. Liao Y, Rao M, Li W, Yang L, Zhu B, Xu R, Fu C (2010) Fumed silica-doped poly (butyl methacrylate-styrene)-based gel polymer electrolyte for lithium ion battery. J Membr Sci 352(1-2):95–99

19. Liang S, Yan W, Wu X, Zhang Y, Zhu Y, Wang H, Wu Y (2018) Gel polymer electrolytes for lithium ion batteries: Fabrication, characterization and performance. Solid State Ionics 318:2–18

20. Deng K, Zeng Q, Wang D, Liu Z, Qiu Z, Zhang Y, Xiao M, Meng Y (2020) Single-ion conducting gel polymer electrolytes: design, preparation and application. J Mater Chem A 8(4):1557–1577

21. Mazuki NF, Kufian MZ, Nagao Y, Samsudin AS (2022) Correlation studies between structural and ionic transport properties of lithium-ion hybrid gel polymer electrolytes based PMMA-PLA. J Polym Environ 30(5):1864–1879

22. Fong KD, Self J, Diederichsen KM, Wood BM, McCloskey BD, Persson KA (2019) Ion transport and the true transference number in nonaqueous polyelectrolyte solutions for lithium ion batteries. ACS Central Science 5(7):1250–1260

23. Zhao X, Tao C-a, Li Y, Chen X, Wang J, Gong H (2020) Preparation of gel polymer electrolyte with high lithium ion transference number using GO as filler and application in lithium battery. Ionics 26:4299–4309

24. Tsao C-H, Su H-M, Huang H-T, Kuo P-L, Teng H (2019) Immobilized cation functional gel polymer electrolytes with high lithium transference number for lithium ion batteries. J Membr Sci 572:382–389

25. Osada I, de Vries H, Scrosati B, Passerini S (2016) Ionic-liquid-based polymer electrolytes for battery applications. Angew Chem Int Ed 55(2):500–513

26. Isikli S, Ryan KM (2020) Recent advances in solid-state polymer electrolytes and innovative ionic liquids based polymer electrolyte systems. Curr Opin Electrochem 21:188–191

27. Ravi M, Kim S, Ran F, Kim DS, Lee YM, Ryou M-H (2021) Hybrid gel polymer electrolyte based on 1-methyl-1-Propylpyrrolidinium Bis (Trifluoromethanesulfonyl) imide for flexible and shape-variant lithium secondary batteries. J Membr Sci 621:119018

28. Perissi I, Caporali S, Fossati A, Lavacchi A (2011) Corrosion resistance of metallic materials in ionic liquids. Adv Chem Res 6:315–322

29. Hayyan M, Ibrahim M, Hayyan A, Hashim MA (2017) Investigating the long-term stability and kinetics of superoxide ion in dimethyl sulfoxide containing ionic liquids and the application of thiophene destruction. Braz J Chem Eng 34:227–239

30. Evans J, Vincent CA, Bruce PG (1987) Electrochemical measurement of transference numbers in polymer electrolytes. Polym 28(13):2324–2328

31. Osman Z, Ghazali MM, Othman L, Isa KM (2012) AC ionic conductivity and DC polarization method of lithium ion transport in PMMA–$LiBF_4$ gel polymer electrolytes. Results in Physics 2:1–4

32. Sa'adun NN, Subramaniam R, Kasi R (2014) Development and characterization of poly (1-vinylpyrrolidone-co-vinyl acetate) copolymer based polymer electrolytes. Sci World J 2014:254215

33. Hashim N, Subban R (2018) Studies on conductivity, structural and thermal properties of PEO-LiTFSI polymer electrolytes doped

with EMImTFSI ionic liquid. In: AIP Conference Proceedings, vol 1. AIP Publishing LLC, p 020021

34. Chew K, Tan K (2011) The effects of ceramic fillers on PMMA-based polymer electrolyte salted with lithium triflate, $LiCF_3SO_3$. Int J Electrochem Sci 6(11):5792–5801

35. Yusuf SNF, Yahya R, Arof AK (2017) Ionic liquid enhancement of polymer electrolyte conductivity and their effects on the performance of electrochemical devices. In: Handy S (ed) Progress and Developments in Ionic Liquids. IntechOpen, London, UK, pp 157–183

36. Mazuki NF, Khairunnisa K, Saadiah MA, Kufian MZ, Samsudin AS (2023) Ionic transport study of hybrid gel polymer electrolyte based on PMMA-PLA incorporated with ionic liquid. Ionics 29(2):625–638

37. Khurana S, Chandra A (2018) Ionic liquid-based organic–inorganic hybrid electrolytes: Impact of in situ obtained and dispersed silica. J Polym Sci, Part B: Polym Phys 56(3):207–218

38. Chaurasia SK, Singh MP, Singh MK, Kumar P, Saroj A (2022) Impact of ionic liquid incorporation on ionic transport and dielectric properties of PEO-lithium salt-based quasi-solid-state electrolytes: role of ion-pairing. J Mater Sci: Mater Electron 33(3):1641–1656

39. Ramesh S, Yahaya AH, Arof AK (2002) Dielectric behaviour of PVC-based polymer electrolytes. Solid State Ionics 152:291–294

40. Rasali N, Saadiah M, Zainuddin N, Nagao Y, Samsudin A (2020) Ionic transport studies of solid bio-polymer electrolytes based on carboxymethyl cellulose doped with ammonium acetate and its potential application as an electrical double layer capacitor. eXPRESS Polym Lett 14(7):619–637

41. Tripathi M, Tripathi SK (2017) Electrical studies on ionic liquid-based gel polymer electrolyte for its application in EDLCs. Ionics 23(10):2735–2746

42. Ramlee F, Farhana N, Bashir S, Saidi NM, Omar FS, Ramesh S, Ramesh K, Ramesh S (2021) Electrical property enhancement of poly (vinyl alcohol-co-ethylene)–based gel polymer electrolyte incorporated with triglyme for electric double-layer capacitors (EDLCs). Ionics 27:361–373

43. Rasali NMJ, Samsudin AS (2017) Ionic transport properties of protonic conducting solid biopolymer electrolytes based on enhanced carboxymethyl cellulose-NH₄Br with glycerol. Ionics 24:1639–1650

44. Gohel K, Kanchan DK (2019) Effect of PC: DEC plasticizers on structural and electrical properties of PVDF–HFP: PMMA based gel polymer electrolyte system. J Mater Sci - Mater Electron 30(13):12260–12268

45. Dissanayake M, Thotawatthage C, Senadeera G, Bandara T, Jayasundara W, Mellander B-E (2013) Efficiency enhancement in dye sensitized solar cells based on PAN gel electrolyte with $Pr_4NI+ MgI_2$ binary iodide salt mixture. J Appl Electrochem 43:891–901

46. Vignarooban K, Badami P, Dissanayake MAKL, Ravirajan P, Kannan AM (2017) Poly-acrylonitrile-based gel-polymer electrolytes for sodium-ion batteries. Ionics 23(10):2817–2822

47. Kumar GG, Sampath S (2003) Electrochemical characterization of poly (vinylidenefluoride)-zinc triflate gel polymer electrolyte and its application in solid-state zinc batteries. Solid State Ionics 160(3-4):289–300

48. Verduzco JC, Vergados JN, Strachan A, Marinero EE (2021) Hybrid polymer-garnet materials for all-solid-state energy storage devices. ACS omega 6(24):15551–15558

49. Singh SK, Gupta H, Balo L, Shalu SVK, Tripathi AK, Verma YL, Singh RK (2018) Electrochemical characterization of ionic liquid based gel polymer electrolyte for lithium battery application. Ionics 24:1895–1906

50. Nath G, Dhapola PS, Sahoo N, Singh S, Singh V, Singh PK (2022) Polyvinylpyrrolidone with ammonium iodide and plasticizer ethylene carbonate solid polymer electrolyte for supercapacitor application. J Thermoplast Compos Mater 35(6):879–890

51. Asnawi A, Hamsan M, Aziz S, Kadir M, Matmin J, Yusof Y (2021) Impregnation of [Emim] Br ionic liquid as plasticizer in biopolymer electrolytes for EDLC application. Electrochim Acta 375:137923

52. Ravi M, Song S, Wang J, Nadimicherla R, Zhang Z (2016) Preparation and characterization of biodegradable poly (ε-caprolactone)-based gel polymer electrolyte films. J Ionics 22(5):661–670

53. Sheng L, Xie X, Sun Z, Zhao M, Gao B, Pan J, Bai Y, Song S, Liu G, Wang T (2021) Role of separator surface polarity in boosting the lithium-ion transport property for a lithium-based battery. ACS Appl Energy 4(5):5212–5221

54. Diederichsen KM, McShane EJ, McCloskey BD (2017) Promising routes to a high Li+ transference number electrolyte for lithium ion batteries. ACS Energy Letters 2(11):2563–2575

55. Liu Y, Zeng Q, Li Z, Chen A, Guan J, Wang H, Wang S, Zhang L (2023) Recent development in topological polymer electrolytes for rechargeable lithium batteries. Adv Sci:2206978

56. RenWei EK (2022) Measurement of lithium transference number in PMMA solid polymer electrolytes doped with micronsized fillers. J Mech Eng Technol (JMET) 13(2):30–42

57. Kufian M, Arof A, Ramesh S (2019) PMMA-LiBOB gel polymer electrolytes in lithium-oxygen cell. In: IOP Conference Series: Materials Science and Engineering, vol 1. IOP Publishing, p 012010

58. Boz B, Ford HO, Salvadori A, Schaefer JL (2021) Porous polymer gel electrolytes influence lithium transference number and cycling in lithium-ion batteries. Electron Mater 2(2):154–173

59. Abarna S, Hirankumar G (2017) Vibrational, electrical, and ion transport properties of PVA-$LiClO_4$-sulfolane electrolyte with high cationic conductivity. Ionics 23:1733–1743

60. Wang Y, Fu L, Shi L, Wang Z, Zhu J, Zhao Y, Yuan S (2019) Gel polymer electrolyte with high Li+ transference number enhancing the cycling stability of lithium anodes. ACS Appl Mater Interfaces 11(5):5168–5175

61. Karuppasamy K, Theerthagiri J, Vikraman D, Yim C-J, Hussain S, Sharma R, Maiyalagan T, Qin J, Kim H-S (2020) Ionic liquid-based electrolytes for energy storage devices: a brief review on their limits and applications. Polym 12(4):918

62. Ghosh A, Wang C, Kofinas P (2010) Block copolymer solid battery electrolyte with high Li-ion transference number. J Electrochem Soc 157(7):A846

63. Appetecchi GB, Croce F, Scrosati B (1995) Kinetics and stability of the lithium electrode in poly (methylmethacrylate)-based gel electrolytes. Electrochim Acta 40(8):991–997

64. Shah DB, Olson KR, Karny A, Mecham SJ, DeSimone JM, Balsara NP (2017) Effect of anion size on conductivity and transference number of perfluoroether electrolytes with lithium salts. J Electrochem Soc 164(14):A3511

65. Li L, Wang J, Yang P, Guo S, Wang H, Yang X, Ma X, Yang S, Wu B (2013) Preparation and characterization of gel polymer electrolytes containing N-butyl-N-methylpyrrolidinium bis (trifluoromethanesulfonyl) imide ionic liquid for lithium ion batteries. Electrochim Acta 88:147–156

66. Li W, Pang Y, Liu J, Liu G, Wang Y, Xia Y (2017) A PEO-based gel polymer electrolyte for lithium ion batteries. RSC Adv 7(38):23494–23501

67. Isa KM, Othman L, Hambali D, Osman Z (2017) Electrical and electrochemical studies on sodium ion-based gel polymer electrolytes. In: AIP Conference Proceedings, vol 1. AIP Publishing LLC, p 040001

68. Wang S, Song H, Song X, Zhu T, Ye Y, Chen J, Yu L, Xu J, Chen K (2021) An extra-wide temperature all-solid-state lithium-metal battery operating from− 73°C to 120°C. Energy Storage Mater 39:139–145

69. Moreno M, Simonetti E, Appetecchi GB, Carewska M, Montanino M, Kim G-T, Loeffler N, Passerini S (2016) Ionic liquid electrolytes for safer lithium batteries. J Electrochem Soc 164(1):A6026

70. Karuppasamy K, Kim H-S, Kim D, Vikraman D, Prasanna K, Kathalingam A, Sharma R, Rhee HW (2017) An enhanced electrochemical and cycling properties of novel boronic ionic liquid based ternary gel polymer electrolytes for rechargeable Li/LiCoO$_2$ cells. Scientific Reports 7(1):1–11

71. Wang Y, Zhong WH (2015) Development of electrolytes towards achieving safe and high-performance energy-storage devices: a review. ChemElectroChem 2(1):22–36

72. Holmberg RJ, Beauchemin D, Jerkiewicz G (2014) Characteristics of colored passive layers on titanium: morphology, optical properties, and corrosion resistance. ACS Appl Mater Interfaces 6(23):21576–21584

73. Chowdhury FI, Khalil I, Khandaker M, Rabbani M, Uddin J, Arof A (2020) Electrochemical and structural characterization of polyacrylonitrile (PAN)–based gel polymer electrolytes blended with tetrabutylammonium iodide for possible application in dye-sensitized solar cells. Ionics 26(9):4737–4746

74. Dose WM, Xu C, Grey CP, De Volder MF (2020) Effect of anode slippage on cathode cutoff potential and degradation mechanisms in Ni-rich Li-ion batteries. Cell Rep Phys Sci 1(11):100253

75. Asenbauer J, Eisenmann T, Kuenzel M, Kazzazi A, Chen Z, Bresser D (2020) The success story of graphite as a lithium-ion anode material–fundamentals, remaining challenges, and recent developments including silicon (oxide) composites. Sustain Energy Fuels 4(11):5387–5416

76. Müller D, Dufaux T, Birke KP (2019) Model-based investigation of porosity profiles in graphite anodes regarding sudden-death and second-life of lithium ion cells. Batteries 5(2):49

77. Vorauer T, Kumar P, Berhaut CL, Chamasemani FF, Jouneau P-H, Aradilla D, Tardif S, Pouget S, Fuchsbichler B, Helfen L (2020) Multi-scale quantification and modeling of aged nanostructured silicon-based composite anodes. Commun Chem 3(1):141

78. Wang A, Kadam S, Li H, Shi S, Qi Y (2018) Review on modeling of the anode solid electrolyte interphase (SEI) for lithium-ion batteries. npj Comput Mater 4(1):15

79. Chatterjee K, Pathak AD, Lakma A, Sharma CS, Sahu KK, Singh AK (2020) Synthesis, characterization and application of a non-flammable dicationic ionic liquid in lithium-ion battery as electrolyte additive. Sci Rep 10(1):9606

80. Liu C, Ma X, Xu F, Zheng L, Zhang H, Feng W, Huang X, Armand M, Nie J, Chen H (2014) Ionic liquid electrolyte of lithium bis (fluorosulfonyl) imide/N-methyl-N-propylpiperidinium bis (fluorosulfonyl) imide for Li/natural graphite cells: Effect of concentration of lithium salt on the physicochemical and electrochemical properties. Electrochim Acta 149:370–385

81. Armand M, Axmann P, Bresser D, Copley M, Edström K, Ekberg C, Guyomard D, Lestriez B, Novák P, Petranikova M (2020) Lithium-ion batteries–current state of the art and anticipated developments. J Power Sources 479:228708

82. Kim D-W (1998) Electrochemical characteristics of a carbon electrode with gel polymer electrolyte for lithium-ion polymer batteries. J Power Sources 76(2):175–179

83. Naderi R, Gurung A, Zhou Z, Varnekar G, Chen K, Zai J, Qian X, Qiao Q (2017) Activation of passive nanofillers in composite polymer electrolyte for higher performance lithium-ion batteries. Adv Sustain Syst 1(8):1700043

84. Ma X, Huang X, Gao J, Zhang S, Deng Z, Suo J (2014) Compliant gel polymer electrolyte based on poly (methyl acrylate-co-acrylonitrile)/poly (vinyl alcohol) for flexible lithium-ion batteries. Electrochim Acta 115:216–222